ANALYSIS OF CARILITE OLIGOMERS AND THEIR FUNCTIONALIZATION WITH FURFURYLAMINE AT LOW CONVERSION BY GPC, NMR AND ESI-MASS SPECTROSCOPIES

CAMILO FLORES-CARRILLO [1], TOSHIMICHI SHIBUE [2], TAKEO SUGA [3], MARIO E. FLORES [1], RANJITA K. BOSE [4], AND IGNACIO MORENO-VILLOSLADA [1]*

[1]*Laboratorio de Polímeros, Instituto de Ciencias Químicas, Facultad de Ciencias, Universidad Austral de Chile, 5090000, Valdivia, Chile.*
[2]*Materials Characterization Central Laboratory, School of Science and Engineering, Waseda University, 3-4-1 Okubo, Shinjuku, Tokyo 169-8555, Japan.*
[3]*Department of Applied Chemistry, School of Science and Engineering, Waseda University, 3-4-1 Okubo, Shinjuku, Tokyo 169-8555, Japan.*
[4]*Engineering and Technology Institute Groningen, University of Groningen, 9747 AG, Groningen, the Netherlands.*

ABSTRACT

Carilite oligomers may be easily functionalized with primary amines, such as furfuryl amine (Fu), through the Paal-Knorr reaction, converting polymeric 1,4-diketone groups into N-substituted pyrroles with pendant furanyl groups. The resulting oligomers allow producing polymer and polymer composites materials by adding a bifunctional dienophile, leading to reversible crosslinking through the Diels-Alder reaction. The extent of conversion in the Paal Knorr reaction should determine the amount of polymer chains showing two or more furanyl dienes, condition necessary for extended crosslinking. Thus, the objectives of this work consisted of i) to characterize a sample of Carilite oligomers (PK_{30}), ii) to calculate the probabilistic distribution of the N-substituted pyrroles in the oligomer chains as a function of the expected diketone conversion, and iii) to compare the prediction with experimental data of a sample obtained after reaction between PK_{30} and Fu aiming at 20 % of conversion ($PK_{30}Fu_{18}$). **Methods**: GPC, NMR, and ESI mass spectroscopies are used for the analysis of the polymers. Poisson distribution and one-dimensional hard-dimer exclusion models have been applied for probabilistic calculations. **Results**: Carilite oligomers are a polydisperse mixture where the most abundant molecules present 1 – 15 ketone moieties. After functionalization, the most abundant derivatized molecules consist of oligomers functionalized with only one Fu residue. Good matching with the predictions were found. **Conclusions:** The use of NMR combined with ESI-mass spectroscopy has served to understand the molecular structure of Carilite oligomers and their Fu-functionalized derivatives. This allows determining refined molecular weights that allow calculating effective conversion aimed and, in combination with the probabilistic predictions, obtaining insights of the expected Fu content per chain, contributing to the improvement of design, handling, and control strategies for reversibly crosslinked polymer matrices.

Keywords: Carilite oligomers; Paal-Knorr reaction; Diels-Alder; reversible crosslinking; polymer matrices.

1. INTRODUCTION

Carilite oligomers are short-chain aliphatic polyketones (PK) composed of ethene, propene, and carbon monoxide (CO) in their backbone, featuring 1,4- and 1,5-diketone groups formed through strict alternating copolymerization of CO with olefins.[1,2] The 1,5-diketone groups appear after propene insertion through positions 1,3 (1,3-mode) while the 1,4-diektone groups are formed through insertion of either ethene or propene in the 1,2- or 2,1-modes. These oligomers are highly reactive with primary amines leading to the formation of pyrrole rings along the polymer backbone via the Paal–Knorr reaction.[3,4] The nitrogen substituent may introduce a wide range of functional pendant groups, and the reaction proceeds with the elimination of water as the only by product.[5]

A useful functionalization has been performed with furfuryl amine (Fu), affording pendant furanyl groups in the oligomer chains.[6,7] These functional groups act as dienes in Diels-Alder / retro-Diels Alder (DA / r-DA) equilibrium reactions. Thus, with the addition of bis-maleimide compounds, which act as bifuncional dienophiles, reversible crosslinking between oligomer chains has been achieved.[8] This property is interesting to generate polymer matrices with self-healing and shape memory properties.[9,10] However, to achieve a convenient crosslinking material for practical applications, the conversion of diketone moieties to substituted pyrroles is an important parameter. Oligomers incorporating two or more Fu acquire a bifunctional character and are prone to produce extended networks. Monofunctional oligomers may tend to chain extension, and unreacted oligomers will not be involved in the crosslinking network. Thus, insufficient bifunctional molecules at low conversion restrict crosslinking and network formation. Conversion efficiencies in the range of 40 – 80 % yield robust thermomechanical performance, such as strength and reprocessability, for applications like adhesives and responsive materials.[6,7] Lower degrees of conversion could result in primarily monofunctional or unreacted oligomers, reducing the probability of bifunctional diene motif formation. This can diminish overall crosslink density, glass transition temperature (T_g), and elasticity compared to higher conversion systems. The oligomer chain length further influences bifunctionality: shorter chains reduce the likelihood of two or more pendant furfuryl groups, particularly under low conversion conditions.[7,11–14]

Although Carilite oligomers are structurally well characterized,[11,14] the impact of low functionalization with Fu on DA crosslinking and the consequent resulting properties is not fully established. In this study, the molecular structure and distribution of Carilite oligomers subjected to Fu functionalization will be investigated by GPC and ^{1}H-NMR and ESI-mass spectroscopies. We will show simulated Fu distribution in the different chains using Poisson distribution and one-dimensional hard-dimer exclusion models to understand the number of Fu incorporated per chain. The predictions will be compared with experimental data. This study provides valuable insights into Carilite oligomers structure and their Fu functionalized derivatives, contributing to the improvement of design, handling, and control strategies for reversibly crosslinked polymer matrices.

2. EXPERIMENTAL

2.1 Materials

The stored aliphatic Carilite oligomers labeled as PK_{30}, donated by Shell, were previously synthesized following a reported procedure.[2] Furfuryl amine (Fu, MW = 97.12 g/mol, purity ≥ 99 %, d = 1.1 g/mL, Sigma Aldrich) was used without further purification. The idealized molecular structure of PK_{30}, Fu, and $PK_{30}Fu_{x'}$ can be seen in Figure 1. Chloroform ($CHCl_3$, purity ≥ 99 %, Sigma Aldrich) and chloroform-d ($CDCl_3$, Sigma-Aldrich) were used as working and ^{1}H-NMR solvents, respectively.

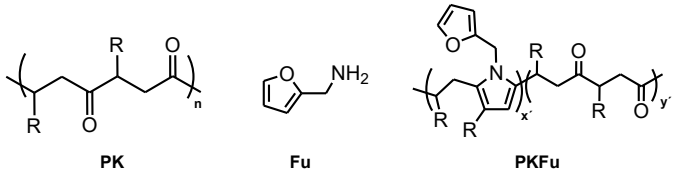

Figure 1. Idealized molecular structures of PK_{30}, Fu, and $PK_{30}Fu_{x'}$. R = H (around 30 %) or CH_3 (around 70 %).

2.2 Equipment

^{1}H-NMR experiments were done in a 400 MHz Mercury Plus (Varian) and in a 600 MHz Avance (Bruker) equipments. Electrospray ionization (ESI) mass spectroscopy was performed in an Exactive Plus (Thermo Fisher Scientific) mass spectrometer. Molecular weight estimations were carried out by gel permeation chromatography (GPC) in a LC-4000 (Jasco) chromatograph, equipped with a RI-4030 refractive index detector (Jasco), and a mixed bed low Jordi Resolve DVB column (Jordi Labs), enclosed at 40 ºC in a CO-4060 column oven (Jasco).

*Corresponding author email: imorenovilloslada@uach.cl

2.3 Procedures

PK_{30} was functionalized using the grafting method employed by Zhang and collaborators.[15] In a typical procedure, 36 g of PK_{30} were weighed and placed in a three-neck round-bottom flask. For this operation, the viscous oligomer was gently heated to around 50 ºC to increase its flowing properties. Once weighed and let cool, 5.54 g of Fu (57 mmol) were incorporated through a drip irrigation system. A reflux system was coupled to the flask, and the reaction was set at 80 ºC vigorously mixing with a Teflon mechanical stirrer. After 3 h, the mixture was let cool down to 40 ºC under stirring, and 100 mL of $CHCl_3$ were added and let mix for 30 min. Then, the reaction mixture was washed by adding 50 mL of deionized water in a separatory funnel. As the final polymer is very viscous and sticky, evaporation of the remaining organic solvent in a rotary evaporator is not recommended. Instead, the organic phase was transferred to a Teflon container and let evaporate under the hood during 24 h. Then, the container with the red viscous polymer was brought to a vacuum chamber at 40 ºC to eliminate the remaining solvent and water, furnished with a $N_{2(l)}$ trap. A total of 30.38 g were obtained (77 % maximum yield).

PK_{30} and the resulting functionalized oligomers were characterized by ^{1}H-NMR, ESI-mass spectroscopies, and GPC. For the former technique, approximately 15 mg of the polymer were dissolved in 2 mL of $CDCl_3$. Each solution was filtered using cotton paper and placed in an NMR tube (inner diameter of 5 mm). The spectra were obtained at room temperature with 32 scans. After characterization of the dicarbonyl conversion to pyrrole units by ^{1}H-NMR, the functionalized oligomer mixture was labelled as $PK_{30}Fu_{18}$. The ESI ion source was operated in positive ion mode, with an ion source temperature of 250 ºC, and N_2 as the nebulizing gas. Methanol solutions containing the oligomers were directly injected into the mass spectrometer at a flow rate of 3 mL / min. A mass range from 100 to 2000 m / z was measured. Data were acquired in profile mode and processed in centroid mode. For GPC analysis, 20 mg of polymeric samples were dissolved with 2.0 mL of THF and stirred in an orbital shaker at 150 rpm overnight. Samples were measured in GPC running with THF as mobile phase at 1 mL / min. Molecular weight estimations (M_w, M_n, and polydispersity index ($Đ$)) were performed with the ChromNAV-GPC software (Jasco), using a molecular weight calibration curve made with different narrow molecular weight poly(methyl methacrylate) (PMMA) standards (ReadyCal Kit, Polymer Standard Service GmbH).

2.4 Data treatment.

The resulting data were analyzed in MestReNova v12 (Mestrelab Research), Ms. Excel (Microsoft), and GraphPad Prism v9 (GraphPad Software), with the aid of the ChatGPT 5.0 IA (Open AI).

From ^{1}H-NMR data, terminal groups and inserted monomers were identified using integral and chemical shift analysis (Equations S1-S8), and their molar fractions were calculated for all the resolved peaks (Equations S9-S14). Then, the ethene (X_e) and propene (X_p) molar fraction in the oligomers could be calculated (Equations S15 and S16) as well as the propene fractions inserted in the 1,3-mode (Equation S17) and the ratio between the resolved end groups (Equations S18).

An average molecular weight of the oligomer chains was calculated in g of polymer / mol of diketone moieties considering ideal polymer chains with infinite length and absence of propene 1,3-insertions (iMW_{dk}, Equations S19 and S20). The average molecular weight of the end groups (MW_{AEG}, Equation S21), an average molecular weight in g of polymer / mol of chains (MW_{PK30}, Equation S22), and the mean number of inserted monomers (Equation S23) were calculated. In addition, a refined, relatively more accurate value for the mean polymer molecular weight in g of polymer / mol of diketone moieties (rMW_{dk}) could be calculated considering end groups and propene 1,3-insertions (Equation S24). For the derivatized $PK_{30}Fu_{18}$ mixture, the degree of conversion was obtained by integral analaysis by ^{1}H-NMR (Equations S25-S31), and the corresponding molecular weight, considering an ideal infinite long chain with no propene 1,3-insertions ($iMW_{PK30Fu18}$) was calculated (Equations S32-S34).

ESI data were treated by filtering the results, once obtaining the C, H, O, and N content and calculating the number of unsaturations or double bond equivalence (DBE), to search for candidate formulae under the following criteria: the adduct ion contains either Na^+ or H^+, the candidate formulas contain only carbon, hydrogen, and oxygen (and nitrogen for $PK_{30}Fu_{18}$); their mass fits within 3 ppm of the theoretical values; they are compatible with reported end groups typical of alternate copolymerization of olefins and CO in the presence of MeOH with Pd catalysts,[2] so that DBE – No. oxygen difference (DBE-O) ranges between -2 and +2; the fraction of ethylene in the chains fits between 0 and 1; for $PK_{30}Fu_{18}$, the number of Fu per chain must be consistent with the content of ketones in original chain. For PK_{30}, the DBE-O allowed calculating the terminal groups and the number of ketone moieties per chain (Equations S35-S40). The molar fraction of ethene in the chains and in the overall sample could also be obtained (Equations S41-S46). Then, the different chains were classified according to the number of ketone groups to calculate their respective frequency and probability to undergo derivatization with Fu. This probability for each chain class was simulated using a Poisson distribution model (Equations S47-S49) and a one-dimensional hard-dimer exclusion model (Equations S50-S51), solved exactly for chains of up to 15 ketone sites, with a single global fugacity (z) numerically adjusted to reproduce the total amine population. Then, ESI data from the experimentally obtained $PK_{30}Fu_{18}$ were analyzed and compared with the predicted results in the simulations. The root mean square error (RMSE) was used to assess quantitative comparisons. Peaks compatible with the transformation of the selected PK_{30} molecules were searched and classified according to the Fu content. Considering their respective frequencies, the incorporation of Fu in the different chains was calculated and compared with the predicted values. In the case of DBE-O = 0 in the PK_{30} analysis, there are two possible end-group pairs: (iso)propenyl carbonyl-methyl ester and alkyl carbonyl-alkyl carbonyl (keto-keto) combinations. When the molecular formulae were compatible with molecules with the two different end-group pairs, calculations were done considering all having one or the other end-group pair. Then, the data split into two. Corresponding series of data were then compared to assess the significance of their differences under the paired t-test. RMSE and the standard deviation of the residuals (SD) were calculated. For other analysis, when differences are found, the results will be given as a data pair (a, b) corresponding to results obtained under the keto-keto or (iso)propenyl carbonyl-methyl ester assumption, respectively.

3. RESULTS AND DISCUSSION

3.1. PK_{30} oligomer mixture characterization by NMR

Figure 2A shows the detailed structure of the PK_{30} oligomers considering a mixture of ethylene and propylene, in which the propylene monomer can be inserted through the 1,2-double bond (1,2- or 2,1-mode) or through the 1,3 position,[2] and a variety of possible end groups as described in the literature.[16] The ^{1}H-NMR spectrum of the PK_{30} oligomers shows six sets of signals in the aliphatic part of the spectrum ranging at 3.5 – 3.7 (**A**), 3.3 – 2.2 (**B**), 2.0 – 1.7 (**C**), 1.65 – 1.45 (**D**), 1.25 – 0.95 (**E**), and 0.95 – 0.8 (**F**) ppm, as can be also seen in Figure 2A. The **A** set corresponds to the CH_3O- methyl ester *o* end groups. The **B** set corresponds to CH_2 and CH protons of both ethylene and propylene units of *x*, *y*, and *z* close to the CO groups, and includes similar protons in the *p*, *q*, and *r* end groups. The **C** set arises as the central methylene of the *z* unit upon 1,3-insertion of propene to the polymer chain,[2] and may also include the methyl of the *s* and *t* end groups. The **D** set is clearly assigned together with the **F** set to both distal methylene and methyl signals, respectively, of the *r* n-propyl end group. The **E** set contains the methyl of the propylene units *y*, and those of the *p* and *q* end groups. In addition, there appears another set of low intense signals in the double bond zone of the spectrum (**G** set) corresponding to =CH and $=CH_2$ in the double bonds of the *s* and *t* end groups (see Figure 2A, inset).

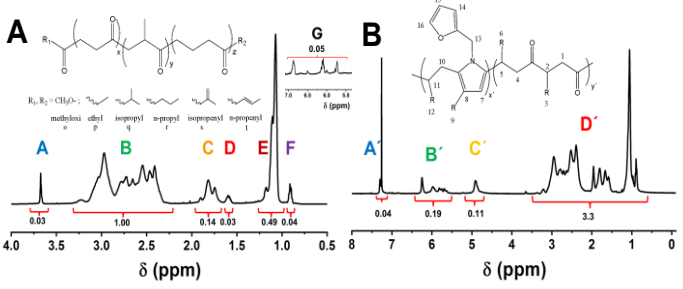

Figure 2. A: 600 MHz ^{1}H-NMR spectrum and a detailed structure of PK_{30}; inset: low intense signals in the double bond zone. **B**: 400 MHz ^{1}H-NMR spectrum and a general structure of $PK_{30}Fu_{18}$.

To further corroborate the assignment, ^{13}C-DEPT NMR and HMQC 2D-NMR analyses have been done (see Figure 3). The negative-phase signals at around 35 – 45 ppm in the DEPT spectrum (Figure 3A) allowed assigning the methylene groups of the aliphatic segments. Complementary ^{1}H – ^{13}C HMQC analysis (Figure 3B) displayed well-defined cross-peaks, confirming the expected chemical connectivity that allows identifying the methyl ester terminal groups of set **A**, the methylenic nature of protons in set **C**, or the combination of methines and methylenes in set **B**.

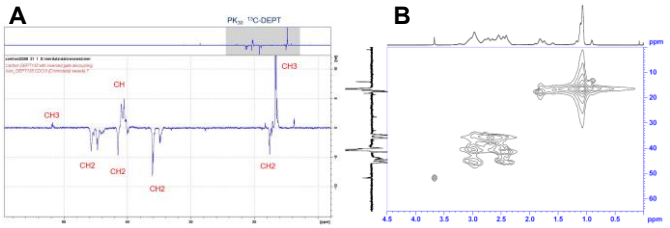

Figure 3. ^{13}C-DEPT (**A**) and HMQC (**B**) spectra of PK_{30}.

From the seven sets of signals in the ^{1}H-NMR spectrum of PK_{30}, we can propose a set of eight equations, among which, the equation corresponding to the **A** set represents its own space, concerning added MeOH, six constitute a set of linearly independent equations, including the normalizing equation, and one is linearly dependent (see Equations S1-S8). Thus, to solve the average composition of the oligomers, we must make assumptions to simplify the number of variables. Due to that *p* and *q* end groups could not be resolved, their contribution, included in the **B** and **E** sets, were assimilated in *x*, *y*, and *z*.

Under this assumption, the ethene / propene ratio in the oligomers resulted 28 : 72 (see Equations S15 and S16). Analysis of the peak integration of the **C** set over the entire spectrum integral shows that the propylene groups inserted in the 1,3-mode represent 14 % of the total propene moieties (see Equation S17), 10 % of the total inserted monomers, lower than the values of 25 – 35 % reported in the literature.[2] The corresponding alkyl carbonyl (keto), (iso)propenyl carbonyl, and methyl ester end groups are found to achieve 40 : 33 : 27 respective ratio.

Here, it must be taken into account that the ethyl and isopropyl end groups, *p* and *q*, respectively, could not be resolved. A molecular weight of 132 g / mol of 1,4-dicarbonyl groups could be calculated considering ideal perfect alternate copolymers of infinite length, ethene / propene ratio of 28 : 72, and the absence of 1,3-insertion of propene ($iMW_{PK30\text{-}dk} = 2MW_k$, see Equations S19-S20). However, this number is underestimated, and unavailable carbonyl groups should be taken into account considering the ester end groups, finiteness of the chains, uneven number of carbonyls in a chain, and the amount of propylene inserted through positions 1,3 giving rise to 1,5-diketones.

The effect of these 1,3-insertions is uncertain, because it depends on their position in the molecular chain (even or odd). Analysis of the peak integration of the **A**, **F**, and **G** sets with respect to that involving **B**, **C**, and **E** sets may allow assuming a 12 mol % of terminal groups, thus concluding a molecular weight (MW_{PK30}) of 1099 g / mol (see Equation S22), and an average of 15 monomers per chain (see Equation S23). In addition, this more refined analysis allows considering end groups and propene 1,3-insertions, neglecting the relative position, to calculate a more realistic molecular weight in g of polymer / mol of diketone units available for the Paal-Knorr reaction, yielding rMW_{dk} = 165 g / mol of 1,4-dicarbonyl groups (Equation (S24)).

3.2. PK_{30} oligomer mixture characterization by GPC

GPC experiments results show retention times that were identified with those of PMMA standards, and M_n = 2066 g / mol, M_w = 5573 g / mol, and M_w/M_n = 2.68 were obtained. The M_n values obtained by GPC are higher than those found with ^{1}H-NMR. GPC often overestimates polymer molecular weight relative to the NMR integration method, especially for low molecular weight polymers, because it provides molecular weight values based on hydrodynamic volume calibration against polymer standards, which may not match the structure of the sample. In contrast, NMR delivers more absolute values determined by direct end-group analysis, thus giving a more accurate result under ideal conditions.[17–19].

3.3. PK_{30} oligomer mixture characterization by ESI-mass spectroscopy

ESI-mass spectra show a distribution of chains centered at around 500 g / mol, with very low intensities beyond 1200 g / mol (see Figure S1). After filtration of data peaks, 332 molecular formula candidates were found whose corresponding peak molecular mass and relative intensity are plotted in Figure 4A. The corresponding chains show alkyl carbonyl (keto), (iso)propenyl carbonyl, and methyl ester end groups at a respective proportion varying from, 67 : 31 : 2 to 58 : 37 : 7 when considering keto-keto or (iso)propenyl carbonyl-methyl ester end-group pair, respectively, if DBE-O = 0. The results considering (iso)propenyl carbonyl-methyl ester end-group pair are more consistent with ^{1}H-NMR results, where the ratio (iso)propenyl carbonyl / and methyl ester end groups is found to be 5:1. The end-group pairs are distributed in molecules containing (iso)propenyl carbonyl-keto (59 %), keto-keto (36 , 27) %, keto-methyl ester (3 %), (iso)propenyl carbonyl-methyl ester (2 , 11) %, and (iso)propenyl carbonyl-(iso)propenyl carbonyl (1 %) end-group pairs. Note that 9 % of the molecules have an ambiguous end-group assignment. Another magnitude calculated is the X_e, of (54 , 49) %, very different from that found by ^{1}H-NMR. It has been pointed out that as polymerization reaction of Carilite oligomers proceeds, the ratio ethene / propene changes. This may cause an imbalance of the ethene / propene ratio in molecular chains with different molecular weight that could impact the ESI-mass results if a fraction of molecules escape from detection.[2] In addition, a higher lability of the methyl ester groups during ionization that could produce molecular fragmentation may also contribute to inconsistencies.[20–23]

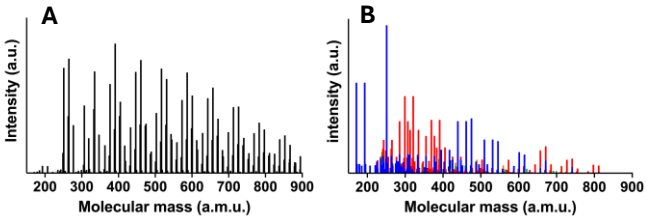

Figure 4. ESI-mass spectra (selected peaks) of PK_{30} (**A**), and $PK_{30}Fu_{18}$ (**B**) showing molecules derivatized with 0 – 5 grafted Fu.

The corresponding compounds present between 1 and 15 ketone groups. This is partially consistent with the ^{1}H-NMR results, which showed 15 monomers as average. As can be seen in Figure 5A, a normal distribution of chains as a function of the number of ketone moieties per chain was obtained, centered at around 7 ketones / chain. This implies that the number of diketone units available for the Paal-Knorr reaction in every chain are equal to or lower than 7, typically 3. The same considerations made above must be done here, concerning the parity of the number of ketone groups, and the number and position of 1,3-insertions of propylene. The probability of a ketone moiety to react with Fu through the Paal-Knorr reaction may depend, then, on the size of the chain. The relative number of ketone moieties belonging to the same class of chain (concerning the number of ketone moieties per chain) is plotted in Figure 5B. The maximum is displaced, indicating that the molecules with 9 ketones per chain are the strongest contributors to the ketone population. Note that these conclusions apply for histograms obtained considering either keto-keto or (iso)propenyl carbonyl-methyl ester end-group pairs, since very similar distributions are found. Analysis of the residuals for each set of data indicates that the differences are not significant ($p > 0.9999$ and $p = 0.2570$), with RMSE of 0.43 and 0.49 % and SD of 0.44 and 0.49 for the distributions shown in Figures 5A and 5B, respectively.

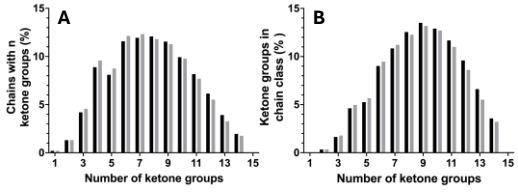

Figure 5. A: Relative frequency of chains containing 1 – 15 ketone groups. **B:** Relative frequency of ketone groups as a function of the number of ketone moieties per chain. **Black** applies for data considering keto-keto end-group pairs and **grey** for data considering (iso)propenyl carbonyl-methyl ester end-group pairs when DBE-O = 0 and the molecular formulae are compatible with both end-group pairs.

3.4. PK_{30} oligomer mixture derivatization with Fu

The probability of reaction of any single Carilite oligomer chain with two or more Fu groups as a function of the degree of conversion of diketones to pyrrole derivatives is of interest to have insights of the crosslinking behavior of the mixture. This probability can be simulated according to different approximations, among which we explore the Poisson distribution and the one-dimensional hard-dimer exclusion models, applied to the set of Carilite oligomers found by ESI. The Poisson distribution assumes independent reactivity for any ketone group, so that the restriction of considering two adjacent ketone moieties, or even two ketones in the same molecule, is not imposed. However, it is recognized sufficient accuracy when conversion is low. The one-dimensional hard-dimer exclusion model enforces local exclusion between adjacent ketone groups, thus resulting more accurate, while remaining computationally tractable. For clarity, for the rest of this work, the data obtained from the molecular distribution that considers (iso)propenyl carbonyl-methyl ester end-group pairs when ambiguity exists is shown, since the data considering keto-keto end group pairs behave very similarly. The results of the simulation shown in Tables S1 and S2 contain the data of the assigned probability of the molecular chains to be functionalized with 0 – 5 Fu molecules as a function of the conversion, analyzed under both models. The distribution of the probabilities shifts to higher degree of grafting as the conversion increases, with implications in the number of molecules achieving polyfunctional characteristics, as can be also seen in Figures 6A and 6B. Under the Poisson distribution model, the data resulted in a more spread distribution than under the one-dimensional hard-dimer exclusion model at conversions higher than 25 %, so that the most probable occupancy event at every conversion analyzed shows a lower frequency in the former than in the latter. In addition, it can be seen in Figure 6C that the probability to find Carilite oligomers with two or more furanyl pendant groups increases with the conversion faster following the one-dimensional hard-dimer exclusion model. However, at low conversion, the differences are small.

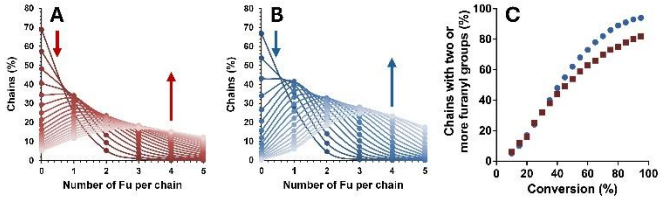

Figure 6. Simulated relative number of chains as a function of the number of furanyl groups per chain for conversion from 10 – 95 % (arrow direction) at increments of 5 % calculated following the Poisson distribution model (**A**) and the one-dimensional hard-dimer exclusion model (**B**). Predicted values of fraction of molecules with two or more grafted Fu, according to the Poisson (■) and one-dimensional hard-dimer exclusion (●) models (**C**).

Analysis of the experiment data by ^{1}H-NMR spectroscopy shows, after derivatization of the PK_{30} Carilite oligomers with Fu, the signals corresponding to the aromatic H16, in α position with respect to the furan oxygen (**A´** set) between 7.5 and 7.0, the rest of the pyrrole and furan aromatic protons (protons H7, H8, H14, and H15) between 7.0 and 5.5 ppm (**B´** set), the methylene group in the Fu residue (H13) between 5.0 – 4.5 ppm (**C´** set), and the methyl groups bound to pyrrole together with the other expected PK_{30} protons (**D´** set) **(**Figure 2B). Integral analyses showed a conversion of PK_{30} diketone groups ($x´$) to derivatized pyrrole moieties of 18 %, both using sets **B´** and **D´**, or **C´** and **D´** for its calculation (see Equation S25 – S31). For this assignment, the polymers have been considered as ideal infinite long chains without propene 1,3-insertions. Thus, the final mixture was labelled $PK_{30}Fu_{18}$. GPC measurements for $PK_{30}Fu_{18}$ show retention times that were identified with those of PMMA standards, and M_n = 2289 g / mol, M_w = 7639 g / mol, and M_w/M_n = 3.34 were obtained.

Analysis of the $PK_{30}Fu_{18}$ by ESI mass spectroscopy showed conversion of most of the 332 molecules found in PK_{30}, although those showing the highest molecular weight were not detected (see Figure 4B). The peaks found are compatible with molecules showing from 0 to 4 pyrrole moieties with furanyl pendant groups. The number of chains classified by their number of converted diketones is plotted in Figures 7A and 7B. The experimental data show 39 % of the molecules with no conversion at all, 50 % with only one Fu molecule, and 8, 2, 1, and 0 % of molecules presenting, respectively, 2, 3, 4, and 5 pyrrole residues, making a total of 11 % of bifunctional chains with two or more furanyl pendant groups. This number is consistent with the values predicted by the simulation of around 16 – 18 % of conversion by both models, as shown in Figure 6C. The distribution of derivatized chains as a function of the number of ketones in each chain is shown in Table 1.

Table 1: Percentage of chains showing n = (0 – 5) Fu grafted to PK_{30} as a function of the number of ketones per chain.

No. ketones per chain	n=0	n=1	n=2	n=3	n=4	n=5
1	5.7	0.0	0.0	0.0	0.0	0.0
2	3.9	3.0	0.0	0.0	0.0	0.0
3	2.8	7.0	0.0	0.0	0.0	0.0
4	7.9	7.7	1.6	0.0	0.0	0.0
5	4.5	12.7	1.4	0.0	0.0	0.0
6	2.1	8.3	1.2	0.5	0.0	0.0
7	5.9	3.7	1.2	0.7	0.0	0.0
8	3.6	2.3	0.9	0.3	0.5	0.0
9	1.4	1.4	0.4	0.3	0.1	0.0
10	0.5	2.2	0.6	0.5	0.0	0.0
11	0.2	1.2	0.5	0.0	0.0	0.0
12	0.0	0.6	0.1	0.0	0.0	0.0
13	0.0	0.0	0.0	0.0	0.0	0.0
14	0.0	0.0	0.0	0.0	0.0	0.0
15	0.0	0.0	0.0	0.0	0.0	0.0

Figure 7A shows, in addition, simulated distribution values at 18 % of conversion by the Poisson and one-dimensional hard-dimer exclusion models. It can be seen in both cases that the most frequent events correspond to molecules showing no derivatization at all, decreasing the frequency as the number of Fu per chain increases. The simulated probability distribution in the different sets of chains, classified by the number of ketone groups present in them, at 18 % of conversion, can be seen in Tables S3 and S4, which show how the probability distributes as the number of ketone groups increases. Comparing the experimental data with the simulated data for conversions from 10 – 95 % at increments of 5 %, we found minimum RMSE values of 8 % at 25 % of conversion under the Poisson approximation, and 5 % obtained at 20 % of conversion by the one-dimensional hard-dimer exclusion model. These values represent a significant deviation, so that the predictive quality is limited. At these conversion values, 25 and 17 % of di- and polyfunctionalized chains were predicted, showing also a deviation of 12 – 4 % with respect to the experimental values. The corresponding simulated distributions at these conversion values are compared to the experimental data in Figure 7B.

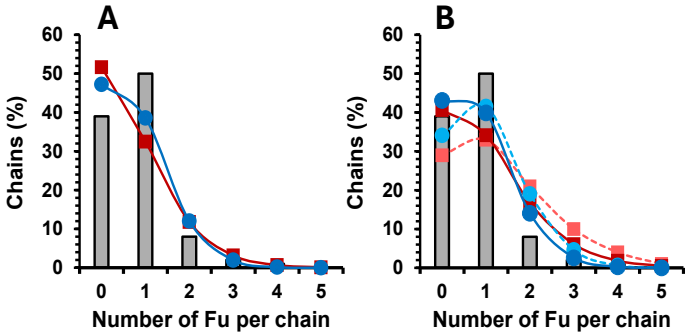

Figure 7. Relative number of chains as a function of the number of furanyl groups. Bars in **A** and **B**: experimental results. Lines in **A:** simulated results at 18 % of conversion under the Poisson distribution (■) and the one-dimensional hard-dimer exclusion (●) models. Lines in **B:** simulated results at 25 (■) and 35 % (■) of conversion under the Poisson distribution model, and at 20 (●) and 25 % (●) of conversion under the one-dimensional hard-dimer exclusion model.

An important feature to analyze in Figures 6A and 6B (and Tables S1 and S2) is the conversion at which the most frequent event shifts from unreacted to monosubstituted chains. In the case of the Poisson distribution model, this occurs between 30 and 35 % of conversion, showing spread values, while in the case of the one-dimensional hard-dimer exclusion model it occurs yet between 20 and 25 % with a higher frequency around the maximum. Then, we search for the conversion values at which the most frequent event is the monofunctionalized chains showing respective differences with the frequencies of the unreacted and bifunctional chains closest to the experimental values (Equation S52). For the Poisson approximation, the best fit occurs at 35 % of conversion, and the probability values are very spread (see Table S5 and Figure 7B). However, with the one-dimensional hard-dimer exclusion model, the best fit is found at conversion of 25 %, where the probabilities concentrate better around the monofunctionalized chains (see Table S6 and Figure 7B). The corresponding di- and polyfunctionalized fraction of molecules calculated at 35 % of conversion under the Poisson distribution model is 38 %, largely overestimated comparing with the experimental value, while under the one-dimensional hard-dimer exclusion model at 25 % of conversion it stood up to 24 %.

3.5. Final analysis and remarks

The distribution of the oligomer chains with respect to the number of Fu incorporated depicted in Figure 7 is compatible with a degree of conversion of 25 – 20 % according to the Poisson distribution and one-dimensional hard-dimer exclusion models, respectively, since, at these conversions, the differences between the simulated values and the experimental data show the lowest RMSE. Considering PK_{30} as an ideal polymer of infinite length and absence of propene 1,3-insertions, an amount of diketone moieties of 273 mmol was calculated with iMW_{dk} = 132 g/mol and the number of mol of Fu in the feed aimed, thus, at 20 % of the diketones. Conversion of 18 %, almost quantitative, is found under the same approximation of an ideal PK_{30} starting material, so that all the PK_{30} proton signal integrals were assimilated to diketone protons. However, with the detailed NMR analysis, where most of the PK_{30} end groups could be resolved, a refined rMW_{dk} = 165 g/mol was calculated, and, thus, the number of mmol of available diketones in the PK_{30} turns into 218 mmol, so the refined Fu molar fraction in the feed changes to 26 % of the more realistically calculated available diketones. Thus, the discrepancy between the ideal conversion derived from NMR (18 %) and the higher apparent conversion suggested by ESI mass spectroscopy and probabilistic simulations (20 – 25 %) stem in considering chain finiteness and propene 1,3-insertions, while the effect of unresolved end groups and the position of the 1,3-insertions (even or odd) seems to average out.

Comparing the predictive quality of both models, the probabilities appear more spread under the Poisson model than under the one-dimensional hard-dimer exclusion model. Spreading the probability has as a result a slightly higher fraction of expected di- and polyfunctional chains at low conversion under the Poisson approximation, while a significant increase of this parameter at high conversion values under the one-dimensional hard-dimer exclusion model occurs. In this case, the Poisson approximation overestimates this parameter more than the one-dimensional hard-dimer exclusion model. Both quantitative and qualitative analysis points at the one-dimensional hard-dimer exclusion model as the best predictor of the experimental data in terms of showing monofunctionalized molecules as the most frequent event, less spread data all through the events, and being compatible with the realistic expected conversion considering the refined rMW_{dk} (25 %).

A large amount of data[3,4,6–10] shows almost quantitative ideal conversion through the Paal-Knorr reaction of Carilite oligomers with primary amines, with slightly decreasing yields as the expected conversion increases, with good reproducibility. The discrepancy between ideal and more realistic available ketone groups may rationally affect the distribution of the grafts along the short oligomer chains. Thus, the number of di- and polyfunctional molecules may be higher than expected considering effective available diketone moieties. At the expected conversion targeted in this work, both models overestimate the fraction of chains containing two or more Fu residues both at the ideal conversion and at the more realistic conversion as compared with the experimental results given by ESI mass spectroscopy (11 %), shifting from 25 – 17 % under ideal considerations to 38 – 24 % under more realistic considerations.

These observations are important to correctly interpret the behavior of the polymers and the materials they conform when using them as polymer matrices where crosslinking plays a major role. Non-grafted molecules do not intervene in crosslinking, whereas monofunctionalized molecules produce chain extension or even capping, minimizing crosslinking. The results found here by ESI mass spectroscopy show a low fraction of molecules undergoing grafting with two or more Fu molecules. The distribution of derivatized chains as a function of the number of ketones in each chain is shown in Table 1. This distribution points at grafted chains possessing between 4 and 12 ketone groups, with growing intensities consistent with their relative frequency depicted in Figure 5. Thus, obtaining di- and polyfunctional derivatized molecules is possible due to that the chain-length distribution is centered around 7 ketones per molecule. However, the fraction of molecules showing less than 4 ketone groups is not negligible, so that, even at high intended conversion, a noticeable fraction of molecules will not integrate the crosslinking network. For applications taking advantage of the reversibility of the DA / r-DA equilibrium, an adequate control of the crosslink density may be pivotal to obtain the desired properties as a function of temperature, so that, sufficient crosslinking density is needed at low temperature to achieve a thermoset behavior, while sufficient effective de-crosslinking must be observed at higher temperature to allow a thermoplastic behavior.

CONCLUSIONS

The molecular structure and distribution of PK_{30} Carilite oligomers and their derivatives obtained at low conversion by the Paal-Knorr reaction ($PK_{30}Fu_{18}$) has been studied by GPC, NMR, and ESI-mass spectroscopies. GPC studies show M_n and M_w of 2066 and 5537 g/mol, respectively, with $Đ$ of 2.68 for PK_{30}, while for $PK_{30}Fu_{18}$ M_n was 2289 g / mol, M_w = 7639 g / mol, and $Đ$ = 3.34. A detailed analysis by NMR allowed distinguishing most end groups from and 1,3-inserted propene from the 1,2-inserted monomers in PK_{30}, so that a refined calculation of the necessary mass to obtain 1 mol of available ketone groups has been done. ESI-mass spectroscopy allowed depicted single chain distribution, and characterization of the end groups, the number of ketone groups per chain (between 1 and 15), and their relative frequency. Once derivatized with Fu, the resulting polymer mixture was also characterized. By ESI-mass spectroscopy, it could be checked that the distribution of the grafted Fu followed the predictions of the one-dimensional hard-dimer exclusion model better than the Poisson probability model. Thus, derivatization of idealized PK_{30} aiming at 20 % of conversion produced polymers with 39 % of unreacted molecules, 50 % of monofunctionalized molecules, and 8, 2, 1, and 0 % of molecules presenting, respectively, 2, 3, 4, and 5 pyrrole residues, making a total of 11 % of polyfunctional chains with two or more furanyl pendant groups. This information is interesting for applications of polymer matrices reversibly crosslinked through the DA / r-DA equilibrium, enabling an adequate control of the crosslink density and the desired properties as a function of temperature, and contributing to the improvement of design, handling, and control strategies.

FUNDING

This work was supported by FONDECYT Regular 1210968 and 1250392 (I.M-V).

REFERENCES

(1) Zhu, L.; Li, J.; Chen, W.-Y.; Ziegler, C. J.; Takahashi, K.; Nozaki, K.; Jia, L. Aliphatic Polyketones from Alternating Copolymerization of CO and Olefins: Phosphinoamidate Nickel Catalyst, Polymerization Study, Mechanical Properties and Degradations. *ACS Appl. Polym. Mater.* **2024**, *6* (16), 9829–9836. https://doi.org/10.1021/acsapm.4c01691.

(2) Mul, W. P.; Dirkzwager, H.; Broekhuis, A. A.; Heeres, H. J.; Van Der Linden, A. J.; Guy Orpen, A. Highly Active, Recyclable Catalyst for the Manufacture of Viscous, Low Molecular Weight, CO–Ethene–Propene-Based Polyketone, Base Component for a New Class of Resins. *Inorganica Chim. Acta* **2002**, *327* (1), 147–159. https://doi.org/10.1016/S0020-1693(01)00697-1.

(3) González Cortes, P.; Araya-Hermosilla, R.; Wrighton-Araneda, K.; Cortés-Arriagada, D.; Picchioni, F.; Yan, F.; Rudolf, P.; Bose, R. K.; Quero, F. Effect of Intermolecular Interactions on the Glass Transition Temperature of Chemically Modified Alternating Polyketones. *Mater. Today Chem.* **2023**, *34*, 101771. https://doi.org/10.1016/j.mtchem.2023.101771.

(4) Toncelli, C.; Schoonhoven, M.-J.; Broekhuis, A. A.; Picchioni, F. Paal-Knorr Kinetics in Waterborne Polyketone-Based Formulations as Modulating Cross-Linking Tool in Electrodeposition Coatings. *Mater. Des.* **2016**, *108*, 718–724. https://doi.org/10.1016/j.matdes.2016.06.127.

(5) Paal-Knorr Pyrrole Synthesis. In *Comprehensive Organic Name Reactions and Reagents*; Wiley, 2010; pp 2107–2110. https://doi.org/10.1002/9780470638859.conrr475.

(6) Araya-Hermosilla, R.; Lima, G. M. R.; Raffa, P.; Fortunato, G.; Pucci, A.; Flores, M. E.; Moreno-Villoslada, I.; Broekhuis, A. A.; Picchioni, F. Intrinsic Self-Healing Thermoset through Covalent and Hydrogen Bonding Interactions. *Eur. Polym. J.* **2016**, *81*, 186–197. https://doi.org/10.1016/j.eurpolymj.2016.06.004.

(7) Araya-Hermosilla, E.; Roscam Abbing, M.; Catalán-Toledo, J.; Oyarzun-Ampuero, F.; Pucci, A.; Raffa, P.; Picchioni, F.; Moreno-Villoslada, I. Synthesis of Tuneable Amphiphilic-Modified Polyketone Polymers, Their Complexes with 5,10,15,20-Tetrakis-(4-Sulfonatophenyl)Porphyrin, and Their Role in the Photooxidation of 1,3,5-Triphenylformazan Confined in Polymeric Nanoparticles. *Polymer* **2019**, *167*, 215–223. https://doi.org/10.1016/j.polymer.2019.01.079.

(8) Orozco, F.; Li, J.; Ezekiel, U.; Niyazov, Z.; Floyd, L.; Lima, G. M. R.; Winkelman, J. G. M.; Moreno-Villoslada, I.; Picchioni, F.; Bose, R. K. Diels-Alder-Based Thermo-Reversibly Crosslinked Polymers: Interplay of Crosslinking Density, Network Mobility, Kinetics and Stereoisomerism. *Eur. Polym. J.* **2020**, *135*, 109882. https://doi.org/10.1016/j.eurpolymj.2020.109882.

(9) Orozco, F.; Kaveh, M.; Santosa, D. S.; Lima, G. M. R.; Gomes, D. R.; Pei, Y.; Araya-Hermosilla, R.; Moreno-Villoslada, I.; Picchioni, F.; Bose, R. K. Electroactive Self-Healing Shape Memory Polymer Composites Based on Diels–Alder Chemistry. *ACS Appl. Polym. Mater.* **2021**, *3* (12), 6147–6156. https://doi.org/10.1021/acsapm.1c00999.

(10) Araya-Hermosilla, E.; Carlotti, M.; Orozco, F.; Lima, G. M. R.; Araya-Hermosilla, R.; Ortega, D. E.; Cortés-Arriagada, D.; Picchioni, F.; Bose, R. K.; Mattoli, V.; Pucci, A. Tailoring Thermomechanical, Shape Memory and Self-Healing Properties of Furan-Based Polyketone via Diels-Alder Chemistry with Different Bismaleimide Crosslinkers. *Polymers* **2025**, *17* (5), 565. https://doi.org/10.3390/polym17050565.

(11) Zhang, W.-L.; Han, S.; Li, S.-H.; Hao, X.-Y.; Lu, X.-B.; Liu, Y. Mechanistic Insights into Cationic [P,O]-Pd-Catalyzed Chain-Transfer Copolymerization of Ethylene with Carbon Monoxide. *Macromolecules* **2024**, *57* (9), 4174–4183. https://doi.org/10.1021/acs.macromol.4c00094.

(12) Gooranorimi, A.; Mousavifard, S. M.; Mohseni, M.; Yahyaei, H.; Makki, H. Effective Cross-Link Density as a Metric for Structure–Property Relationships in Complex Polymer Networks: Insights from Acrylic Melamine Systems. *ACS Appl. Polym. Mater.* **2025**, *7* (14), 9034–9044. https://doi.org/10.1021/acsapm.5c01155.

(13) Torres-Knoop, A.; Schamboeck, V.; Govindarajan, N.; Iedema, P. D.; Kryven, I. Effect of Different Monomer Precursors with Identical Functionality on the Properties of the Polymer Network. *Commun. Mater.* **2021**, *2* (1), 50. https://doi.org/10.1038/s43246-021-00154-x.

(14) Malinova, V.; Rieger, B. Synthesis of Functional Poly(1,4-Ketone)s Bearing Bioactive Moieties by Pd-Catalyzed Insertion Polymerization. *Biomacromolecules* **2006**, *7* (11), 2931–2936. https://doi.org/10.1021/bm0606364.

(15) Zhang, Y.; Broekhuis, A. A.; Picchioni, F. Thermally Self-Healing Polymeric Materials: The Next Step to Recycling Thermoset Polymers? *Macromolecules* **2009**, *42* (6), 1906–1912. https://doi.org/10.1021/ma8027672.

(16) Drent, E.; Budzelaar, P. H. M. Palladium-Catalyzed Alternating Copolymerization of Alkenes and Carbon Monoxide. *Chem. Rev.* **1996**, *96* (2), 663–682. https://doi.org/10.1021/cr940282j.

(17) Gody, G.; Zetterlund, P. B.; Perrier, S.; Harrisson, S. The Limits of Precision Monomer Placement in Chain Growth Polymerization. *Nat. Commun.* **2016**, *7* (1), 10514. https://doi.org/10.1038/ncomms10514.

(18) Izunobi, J. U.; Higginbotham, C. L. Polymer Molecular Weight Analysis by ^{1}H NMR Spectroscopy. *J. Chem. Educ.* **2011**, *88* (8), 1098–1104. https://doi.org/10.1021/ed100461v.

(19) Siddiqui, M. N.; Ali, M. F. Investigation of Chemical Transformations by NMR and GPC during the Laboratory Aging of Arabian Asphalt. *Fuel* **1999**, *78* (12), 1407–1416. https://doi.org/10.1016/S0016-2361(99)00080-0.

(20) Bruns, H.; Ziesche, L.; Taniwal, N. K.; Wolter, L.; Brinkhoff, T.; Herrmann, J.; Müller, R.; Schulz, S. *N* -Acylated Amino Acid Methyl Esters from Marine *Roseobacter* Group Bacteria. *Beilstein J. Org. Chem.* **2018**, *14*, 2964–2973. https://doi.org/10.3762/bjoc.14.276.

(21) Demarque, D. P.; Crotti, A. E. M.; Vessecchi, R.; Lopes, J. L. C.; Lopes, N. P. Fragmentation Reactions Using Electrospray Ionization Mass Spectrometry: An Important Tool for the Structural Elucidation and Characterization of Synthetic and Natural Products. *Nat. Prod. Rep.* **2016**, *33* (3), 432–455. https://doi.org/10.1039/C5NP00073D.

(22) Grossert, J. S.; Fancy, P. D.; White, R. L. Fragmentation Pathways of Negative Ions Produced by Electrospray Ionization of Acyclic Dicarboxylic Acids and Derivatives. *Can. J. Chem.* **2005**, *83* (11), 1878–1890. https://doi.org/10.1139/v05-214.

(23) Mutenda, K. E.; Körner, R.; Christensen, T. M. I. E.; Mikkelsen, J.; Roepstorff, P. Application of Mass Spectrometry to Determine the Activity and Specificity of Pectin Lyase A. *Carbohydr. Res.* **2002**, *337* (13), 1217–1227. https://doi.org/10.1016/S0008-6215(02)00127-1.